Tunable multiferroic properties in nanocomposite $PbTiO_3$–$CoFe_2O_4$ epitaxial thin films

M. Murakami, K.-S. Chang, M. A. Aronova, C.-L. Lin, Ming H. Yu, J. Hattrick Simpers, M. Wuttig, and I. Takeuchi[a)]
Department of Materials Science and Engineering and Center for Superconducting Research, University of Maryland, College Park, Maryland 20742

C. Gao and B. Hu
National Synchrotron Radiation Laboratory and Structure Research Laboratory, University of Science and Technology of China, Hefei, Anhui 230029, China

S. E. Lofland
Department of Physics and Astronomy, Rowan University, Glassboro, New Jersey 08028

L. A. Knauss
Neocera, Inc., 10000 Virginia Manor Road, Beltsville, Maryland 20705

L. A. Bendersky
NIST, Gaithersburg, Maryland 20899

(Received 26 April 2005; accepted 19 July 2005; published online 6 September 2005)

We report on the synthesis of $PbTiO_3$–$CoFe_2O_4$ multiferroic nanocomposites and continuous tuning of their ferroelectric and magnetic properties as a function of the average composition on thin-film composition spreads. The highest dielectric constant and nonlinear dielectric signal was observed at $(PbTiO_3)_{85}$–$(CoFe_2O_4)_{15}$, where robust magnetism was also observed. Transmission electron microscopy revealed a pancake-shaped epitaxial nanostructure of $PbTiO_3$ on the order of 30 nm embedded in the matrix of $CoFe_2O_4$ at this composition. Composition dependent ferroics properties observed here indicate that there is considerable interdiffusion of cations into each other. © *2005 American Institute of Physics*. [DOI: 10.1063/1.2041825]

Multiferroic materials are of significant scientific and technological interests.[1–4] In particular, composite multiferroics can exhibit sizable magnetoelectric (ME) coupling at room temperature,[5,6] and therefore they have the potential for novel device applications such as sensitive magnetic field sensors.[4,7–9] In such systems, the ME effect arises from the elastic coupling between the piezoproperties of the ferromagnetic and ferroelectric components. There have been a number of reports on $BaTiO_3$(BTO)–$CoFe_2O_4$(CFO) multiferroic composites and related materials.[6,10] In these composite systems, eutectic separation of CFO and BTO give rise to the segregation of the two phases. Pursuing such materials in thin film structures is desirable because they offer the possibility to create compositions where the component materials are modulated and coupled at the nanometer level.[10–12]

Previously, we have reported on investigation of thin film multiferroic compounds in BTO–CFO composition spreads where we identified a composition region which was ferromagnetic and displayed a relatively high dielectric constant at room temperature.[10] In this letter, we report on the microstructure and tunable multiferroic properties of CFO–$PbTiO_3$(PTO) thin film composition spreads.

In order to create composition spread structures modulated at the nanometer level, we deposited CFO and PTO by laser ablation in the "superlattice spread" geometry where the wedge thickness of each layer equals multiples of the lattice constants of CFO and PTO (Fig. 1).[13,14] The resulting average composition of the spread varies continuously form pure PTO at one end to pure CFO at the other. The detail of the spread synthesis is described in Ref. 10. (100) MgO substrates were used. The deposition substrate temperature was 600 °C and the oxygen partial pressure was 65 mTorr. The ablation energy was approximately 2 J/cm^2, and the total thickness at each position on the spread was 300 nm. The sample was approximately 6 mm long in the spread direction.

We have found that by varying the layering configuration and the deposition condition, a variety of different nanocomposite configurations can be obtained. Cross-sectional high-resolution transmission electron microscopy (TEM) was performed at different compositions on various spreads. Figure 2(a) was taken from a spot on a spread where the average composition was approximately 80% PTO and 20% CFO (PTO_{80}–CFO_{20}). The wedge thickness of each depos-

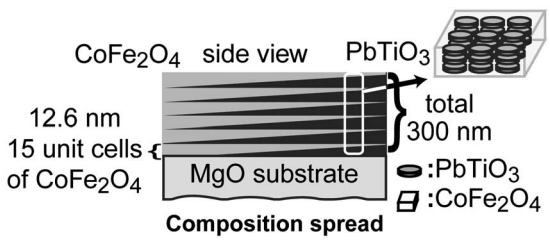

FIG. 1. $CoFe_2O_4$ (CFO)–$PbTiO_3$ (PTO) superlattice composition spreads used to design a magnetoelectric material. The schematic of the composition spread. The thickness of each wedge is 12.6 nm corresponding to 15 unit cells of CFO. The average composition of the film is continuously varied from pure PTO (right) to pure CFO (left). The total thickness of 300 nm is constant across the spread. The boxed region near the composition of PTO_{80}–CFO_{20} was found to be consisting of epitaxial PTO nanopancakes embedded in the CFO matrix.

[a)]Electronic mail: takeuchi@umd.edu

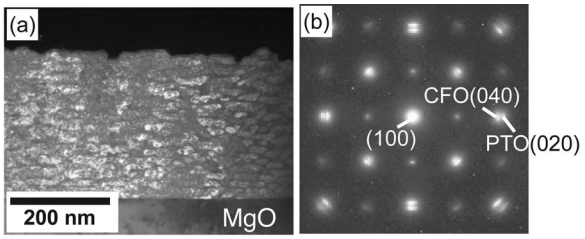

FIG. 2. Cross-sectional high-resolution transmission electron microscopy image (a), and diffraction (b), of $PTO_{80}-CFO_{20}$ region (incident of electron beam is ⟨100⟩ of MgO).

ited layer for this particular spread was 12.6 nm which correspond to roughly 15 unit cells of CFO and 30 units cells of PTO. Pancake-shaped nanostructures of PTO on the order of 30 nm are seen as embedded in the matrix of CFO. In other samples, we have observed structures where one component has formed an ordered array of nanopillars in the matrix of the other component as well as structures where the superlattice configurations have remained intact.[14,15] It is interesting to note that even though we fabricated our samples in a layered manner, the resulting structures have revealed very a different microstructure.

The lattice constants of the end compounds are $a=0.839$ nm for CFO (cubic spinel, $Fd3m$) and $a=0.390$ nm and $c=0.415$ nm for PTO (low-temperature pseudocubic peroveskite, tetragonal $P4mm$), and they are expected to grow heteroepitaxially with the MgO substrate (cubic rocksalt, $Fm3m$, $a=0.421$ nm). Figure 2(b) shows the electron diffraction of the same sample as Fig. 2(a) taken along the (100) direction of MgO. Cubic-like PTO and CFO are clearly observed to have an epitaxial relationship $\langle 100\rangle_{MgO}\|\langle 100\rangle_{PTO}\|\langle 100\rangle_{CFO}$. Although the phase diagram for PTO–CFO is not known, by analogy with $BaTiO_3$ we expect pseudobinary eutectic separation.[6] The nonequilibrium laser deposition process used here together with the nucleation of phases and the eutectic separation is expected to give rise to complex nanostructures. Details of the dependence of the microstructure on various parameters will be published elsewhere.[15]

Figure 3 shows the mapping of ferromagnetic and ferroelectric properties of a CFO–PTO spread with the same layering scheme as the one used to make the sample shown in Fig. 2. The out-of-plane and in-plane remanent magnetization were used as measures of ferromagnetism and determined as a function of average composition using a room-temperature scanning superconducting quantum interference device (SQUID) microscope [Fig. 3(a)]. The magnetization value is defined here as the magnetic moment per film volume. At the pure CFO end, the film is out-of-plane magnetized.[16] As a small amount of PTO is introduced in the structure, there is a sudden increase in in-plane magnetization indicating a drastic change in anisotropy. We attribute this to the diffusion of Pb and Ti ions into CFO leading to a metastable solid solution and the subsequent change in magnetocrystalline anisotropy as well as the microstructure of the material. TEM of this region showed CFO layers to be separated by the nanopancake structure of PTO.[17] Despite the decaying trend in the overall magnetization as more PTO is added, we find that the material remains ferromagnetic toward the low CFO concentration region. The inset of Fig. 3(a) shows a SQUID magnetometer measurement of an individually prepared $PTO_{80}-CFO_{20}$ thin film sample made in the same layer-by-layer manner as described earlier with the field applied in the out-of-plane direction. It shows the presence of robust magnetism despite the reduced overall magnetization at this composition. We have also performed high temperature vibrating sample magnetometer measurement on several individual samples and found that the ferromagnetic Curie temperature is the same for the samples with different average compositions.

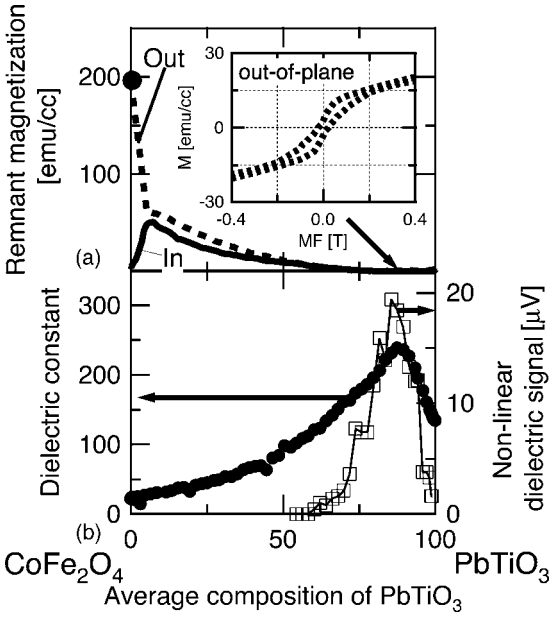

FIG. 3. Magnetic and dielectric properties of the spread at room temperature. (a) In plane (solid line) and out-of-plane (dotted line) remnant magnetization mapping obtained by a scanning SQUID microscope. The inset is a magnetic hysteresis (out-of-plane) of an individual $PTO_{80}-CFO_{20}$ sample. (b) Dielectric constant (left and dots) and nonlinear dielectric signal proportional to $\partial\varepsilon/\partial E$ (right and open square) mapping obtained by a microwave microscope at 1 GHz as a function of average composition across the spread.

The linear dielectric constant ε and the nonlinear dielectric signal were measured across the spread using a scanning microwave microscope operating at 1 GHz [Fig. 3(b)].[18,19] The nonlinear signal here represents the tunability of the dielectric constant $\delta\varepsilon/\delta E$, which is measured as $\delta f_r/\delta E$, where δf_r is the change in the resonant frequency of the microwave microscope cavity due to the applied electric field E in the vertical direction due to a voltage $V_{\text{tip-substrate}}$ applied between the microscope tip and an electrode on the back of the sample substrate.[19] For the present measurement, the amplitude of this ac voltage was 16 V.[18,19]

Overall, both the linear dielectric constant and the nonlinear dielectric signal show a decreasing trend toward the low PTO concentration as expected. However, they display an unexpected peak at approximately $PTO_{85}-CFO_{15}$. To understand this behavior, we performed scanning x-ray microdiffraction (using a D8 DISCOVER with GADDS for combinatorial screening by Bruker-AXS). Figure 3(a) shows the x-ray diffraction spectra taken at room temperature with a 500 μm diameter beam in the 2θ range which includes the PTO (200) and (002) peaks in the composition range of PTO to $PTO_{70}-CFO_{30}$. Continuous shifts in the peaks are observed as a function of the average composition, and the peaks appear to merge at the composition of $PTO_{85}-CFO_{15}$ indicating the occurrence of a structural transition. The lat-

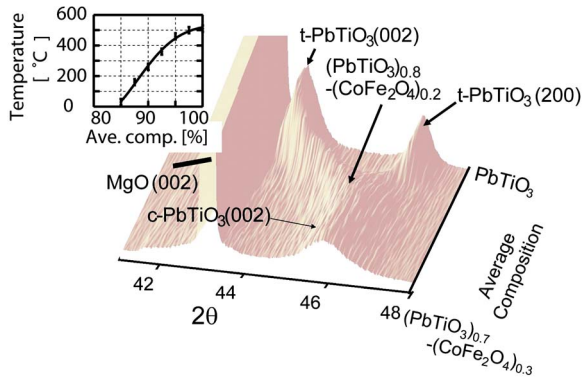

FIG. 4. Structural changes across the spread. (a) X-ray microdiffraction of the $PbTiO_3$-rich side of the spread sample. Upon introducing $CoFe_2O_4$, the (200) and (002) reflections of the twined tetragonal $PbTiO_3$ are seen to continuously shift and eventually merge at $2\theta=45.8°$. Inset shows the continuous shift in this phase transition temperature as a function of the composition across the spread.

tice constant of this composition is in good agreement with the lattice constant of the cubic phase of pure PTO. Thus, the peaks in the room temperature dielectric properties can be identified as the composition where the PTO phase is undergoing a cubic to tetragonal transition at room temperature. We have also performed variable temperature scanning microdiffraction to confirm that the transition temperature (defined to be the temperature at which the tetragonal peaks merge) shifts continuously across the spread in this composition region [Fig. 3(b)]. Based on the fact that we see enhanced dielectric properties and the structural change, we associate this transition to be the ferroelectric Curie temperature. Thus, composition near $PTO_{85}-CFO_{15}$ has optimum biferroic properties: it shows substantial magnetism, while displaying the onset of ferroelectricity and peaking of the piezoelectric coefficient .[20]

There are several factors that could give rise to the continuous shift in the transition temperature as a function of the composition. In epitaxial nanocomposite geometries, the mechanical interaction between the components is known to introduce stress in each other, resulting in a shift in the Curie temperature.[21] But the observed shift from T_C (pure PTO) $\sim 500\ °C$ down to near room temperature is substantial, and stress itself cannot be used to explain such a large shift (Fig. 4). Another possibility is the ferroelectric size effect in our nanometer-sized PTO grains.[22] However, the TEM micrograph of the $PTO_{80}-CFO_{20}$ (where the Curie temperature approximately equals room temperature) region seen in Fig. 2(a) clearly shows the grain size to be of the order of 30 nm. According to the literature, one would not expect to see a significantly reduced T_C until the grain size decreases down to about 20 nm.[23] This is in clear contrast to the microstructure in our nanocomposite.

We believe the dominant effect giving rise to the shift in T_C is the diffusion of Fe and Co ions into PTO leading to a metastable solid solution. In such a solid solution system, T_C can be dramatically affected by even small additions of solute atoms.[24,25] TEM of a $PTO_{95}-CFO_5$ thin film from the spread has shown it to be a single tetragonal phase, although x-ray diffraction of a bulk $PTO_{95}-CFO_5$ sample we made has revealed a trace of CFO with shifts in the PTO peaks. Because of the complex nonequilibrium nature of our nanocomposite growth process, it is not unreasonable to expect a continuous cation substitution between PTO and CFO across the spread well into the region where the separated CFO matrix is clearly also present. We found this shift in the transition temperature to be highly reproducible from sample to sample.

Further investigation of the interdiffusion near the CFO/PTO interfaces is currently underway. The result of the ME effect measurement will be published elsewhere.[26]

This work was supported by ONR N000140110761, ONR N000140410085, NSF DMR 0094265 (CAREER), NSF DMR 0231291, and MRSEC DMR-00-80008.

[1] M. Fiebig, Th. Lottermoser, D. Fröhlich, A. V. Goltsev, and R. V. Pisarev, Nature (London) **419**, 818 (2002).
[2] N. Hur, S. Park, P. A. Sharma, J. S. Ahn, S. Guha, and S.-W. Cheong, Nature (London) **429**, 392 (2004).
[3] B. B. Van Aken, T. T. M. Palstra, A. Filippetti, and N. A. Spaldin, Nat. Mater. **3**, 164 (2004).
[4] S. Dong, J. Cheng, J. F. Li, and D. Viehland, Appl. Phys. Lett. **83**, 4812 (2003).
[5] G. Srinivasan, E. T. Rasmussen, B. J. Levin, and R. Hayes, Phys. Rev. B **65**, 134402 (2002).
[6] J. Van Den Boomgaard, D. R. Terrell, R. A. J. Born, and H. F. J. I Giller, J. Mater. Sci. **9**, 1705 (1974).
[7] N. A. Hill, J. Phys. Chem. B **104**, 6694 (2000).
[8] D. A. Filippov, M. I. Bichurin, V. M. Laletin, and G. Srinivasan, Phys. Solid State **46**, 1674 (2004).
[9] J. Ryu, A. V. Carazo, K. Uchino, and H.-E. Kim, Jpn. J. Appl. Phys., Part 1 **40**, 4948 (2001).
[10] K. S. Chang, M. A. Aronova, C.-L. Lin, M. Murakami, M.-H. Yu, J. Hattrick Simpers, O. O. Famodu, S. Y. Lee, R. Ramesh, M. Wuttig, I. Takeuchi, C. Gao, and L. A. Bendersky, Appl. Phys. Lett. **79**, 4411 (2001).
[11] H. Zheng, J. Wang, S. E. Lofland, Z. Ma, L. Mohaddes-Ardabili, T. Zhao, T. Salamanca-Riba, S. R. Shinde, S. B. Ogale, F. Bai, D. Viehland, Y. Jia, D. G. Schlom, M. Wuttig, A. Roytburd, and R. Ramesh, Science **303**, 661 (2003).
[12] J. G. Wan, X. W. Wang, Y. J. Wu, M. Zeng, Y. Wang, H. Jiang, and W. Q. Zhou, Appl. Phys. Lett. **86**, 122501 (2005).
[13] T. Fukumura, M. Ohtani, M. Kawasaki, Y. Okimoto, T. Kageyama, T. Koida, T. Hasegawa, Y. Tokura, and H. Koinuma, Appl. Phys. Lett. **77**, 3246 (2000).
[14] K.-S. Chang, O. Famodu, I. Takeuchi, S. E. Lofland, J. Hattrick-Simpers, and H. Chang, Appl. Phys. Lett. **79**, 4411 (2001).
[15] L. A. Bendersky (unpublished).
[16] Y. Suzuki, G. Hu, R. B. van Dover, and R. J. Cava, J. Magn. Magn. Mater. **191**, 1 (1999).
[17] M. A. Aronova, Ph.D. thesis, University of Maryland (2004).
[18] C. Gao and X.-D. Xiang, Rev. Sci. Instrum. **69**, 3846 (1998).
[19] C. Gao, F. Duewer, Y. Lu, and X.-D. Xiang, Appl. Phys. Lett. **73**, 1146 (1998).
[20] M. E. Lines and A. M. Glass, *Principles and Applications of Ferroelectrics and Related Materials* (Oxford University Press, New York, 1977).
[21] V. Moshnyaga, B. Famaschke, O. Shapoval, A. Belenchuk, J. Faupel, O. I. Lebedev, J. Verbeeck, G. Van Tendeloo, M. Mücksch, V. Tsurkan, and R. Tidecks, Nat. Mater. **2**, 247 (2003).
[22] A. Roelofs, T. Schneller, K. Szot, and R. Waser, Appl. Phys. Lett. **81**, 5231 (2002).
[23] K. Ishikawa, T. Nomura, N. Okada, and K. Takada, Jpn. J. Appl. Phys., Part 1 **35**, 5196 (1996).
[24] R. E. Eitel, C. A. Randall, T. R. Shrout, P. W. Rehrig, W. Hackenberger, and S.-E. Park, Jpn. J. Appl. Phys., Part 1 **40**, 5999 (2001).
[25] V. V. Lemanov, Phys. Solid State **39**, 1468 (1997).
[26] C. Gao, B. Hu, X. Li, C. Liu, M. Murakami, K.-S. Chang, C. J. Long, M. Wuttig, and I. Takeuchi (unpublished).